



# Helium detection using a planar integrated micro-mass spectrometer

M. Reinhardt\*, G. Quiring, R.M. Ramírez Wong, H. Wehrs, J. Müller

TUHH – Institut für Mikrosystemtechnik, Eißendorferstrasse 42, Raum 1506, 21073 Hamburg, Germany

## ARTICLE INFO

### Article history:

Received 10 February 2010  
Received in revised form 12 May 2010  
Accepted 12 May 2010  
Available online 4 June 2010

### Keywords:

Micro-mass spectrometer  
PIMMS  
Detection limit  
Helium Leak detection  
MEMS  
Synchronous ion shield

## ABSTRACT

A planar integrated micro-mass spectrometer (PIMMS) is presented, which shifts the limit of the measurable range from  $m/z$  12–1206 down to  $m/z$  3–301 compared to results obtained earlier. This shift is achieved by doubling the width of the electrodes of the synchronous ion shield (SIS) mass analyzer. This is confirmed by the detection of helium with the micro-mass spectrometer, which allows its use for helium leak detection. The introduction of a micro-channel plate improves the sensitivity of the PIMMS to <400 ppm.

© 2010 Elsevier B.V. All rights reserved.

## 1. Introduction

One of the present objectives in mass spectrometry is to reduce the size of mass spectrometers. The main reason for miniaturization is the application of mass spectrometry in fields where current technologies are hardly feasible due to environmental, physical or cost constraints. The pursuit of this goal has led to the exploration of alternative manufacturing techniques such as microsystems technologies. The small mass of a miniature device enhances its robustness against shock and vibrations. Such devices consume only a fraction of power of conventional equipment. The vacuum requirements are significantly relaxed, since the needed ion mean free path scales with size. Moreover, if appropriate micromachining fabrication processes are used, such miniaturized devices can be produced at much lower costs. These advantages in combination with the mobility of the device open a new range of applications for mass spectrometry such as in situ and online monitoring in harsh environments.

Different approaches for the miniaturization of mass spectrometers have been undertaken. One of them is the size reduction of ion traps by using micromachining, and toroidal and hyperbolic profiles have been investigated [1–3]. The miniaturization of sector devices by using standard machining methods and thin film photolithographic techniques has been reported [4], where  $m/z$  separation is accomplished by superimposed magnetic and electric fields. Miniaturized quadrupoles have been reported using MEMS

technologies [5,6]. More recently, quadrupole electrodes have been fabricated by rapid prototyping techniques [7], which allowed optimizing the resolution of the measured spectra. Such a device is able to measure in the range  $m/z$  1–10, which makes it technologically relevant (for applications such as a helium leak detection device). Still, issues such as temperature stability have to be addressed.

Previously, a fully integrated micro-mass spectrometer has been presented where all components of a mass spectrometer are integrated by using MEMS technologies [8,9]. It incorporates a novel synchronous ion shield (SIS) mass analyzer. The relevant potential distributions (time-invariant fields) and the SIS operation principle (time-variant fields) have been evaluated by numerical simulations and verified experimentally [10].

In this paper, results of the characterization of this SIS mass analyzer are presented, with the focus of making a smaller scan range accessible starting at  $m/z$  3. The necessary modifications of the existing planar integrated micro-mass spectrometer (PIMMS) are described and theoretical results are given. The resulting spectral range allows helium detection, which is demonstrated with a gas sample.

## 2. Theory of operation

An ion source, an ion separation device and a detector are components of a classical mass spectrometer. The planar integrated micro-mass spectrometer integrates on-chip all these components using MEMS technologies. An overview of the PIMMS geometry is shown in Fig. 1.

The electron source, ionization chamber and ion optics are combined to form the ion source. The sample gas is brought to the ionization chamber via a system of capillaries. There, it is ionized

\* Corresponding author. Tel.: +49 4042 878 2334.

E-mail address: [reinhardt@tu-harburg.de](mailto:reinhardt@tu-harburg.de) (M. Reinhardt).

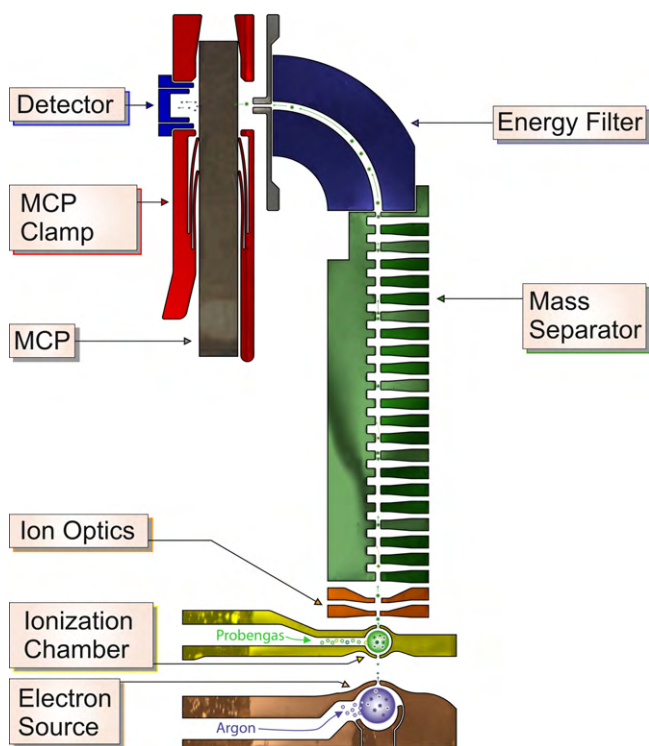


**Fig. 1.** Overview of the PIMMS. All components are batch manufactured using MEMS technologies. The MCP is manually integrated after manufacturing.

by electron ionization. On-chip micro-plasma serves as the electron source. A noble gas is used as plasma gas (usually Ar, but also Kr or Xe are used). The extracted ions are accelerated to a defined energy and focused to a parallel ion beam into the SIS mass analyzer.

The SIS mass analyzer allows ions with a specific velocity to pass through it. This velocity is given by the frequency of the rectangular shaped signals driving the separator. The SIS consists of 20 finger electrodes and a comb structure which build the analyzer channel. A potential difference between a finger electrode and the comb structure leads to an electric field that is direct perpendicular to the ion movement direction. An ion which is subjected to such a field for long enough will be deflected to the side of the separator

and will not reach the next stage. By driving the finger electrodes with time variant rectangular shaped signals it is possible to move a field-free region along the channel at the speed of the ions to be isolated. Ions with the proper speed will pass the separator in the field-free regions. They are shielded from the deflecting fields. A frequency sweep of the signals driving the SIS allows to record spectra.

Since ions might gain or lose kinetic energy due to fringing fields in the separator or thermal scattering in the ionization chamber, an energy filter is placed behind the mass analyzer. This sector field filters the ions according to their kinetic energy. This is crucial for the detection of the correct  $m/z$ .

After separation, the ion current is in the range of a few picoamperes. To enhance the sensitivity of PIMMS, a micro-channel plate (MCP) is inserted into the ion flight path. The electrons emitted by the MCP are detected by the Faraday cup. A highly sensitive current amplifier is implemented close to the PIMMS chip.

### 3. Detecting helium

The signals represented in the path-time-field diagram shown in Fig. 2a are generated by a signal generator which was specifically designed for driving the SIS mass analyzer of PIMMS. It generates four rectangular shaped signals, phase-shifted by  $90^\circ$  and with duty cycle of 25% in range of 5–50 MHz. The SIS consists of 20 finger electrodes, where four neighbored finger electrodes are connected to four different signals, so that every signal is connected to five finger electrodes.

The relationship which governs the selection of the  $m/z$  of the ions with the frequency  $f$  of the signals driving the SIS mass analyzer is:

$$zU = \frac{1}{2}mv^2 \Rightarrow \frac{m}{z} = \frac{2U}{(df)^2},$$

where  $z$  is the charge of the ion,  $U$  the ion acceleration voltage and  $d$  the distance between two finger electrodes of the separator driven by the same signal. That means in the experiment of Fig. 2a that  $d$  equals the width of four finger electrodes. As an example, the width of the electrodes and the gap between them is  $100 \mu\text{m}$ , hence  $d_a = 800 \mu\text{m}$ , in this special case the width of an electrode is the same as the width of a finger electrode. In Fig. 2b the electrode width is tripled to  $300 \mu\text{m}$  (two finger electrodes and one gap) such that  $d_b = 1600 \mu\text{m}$ .

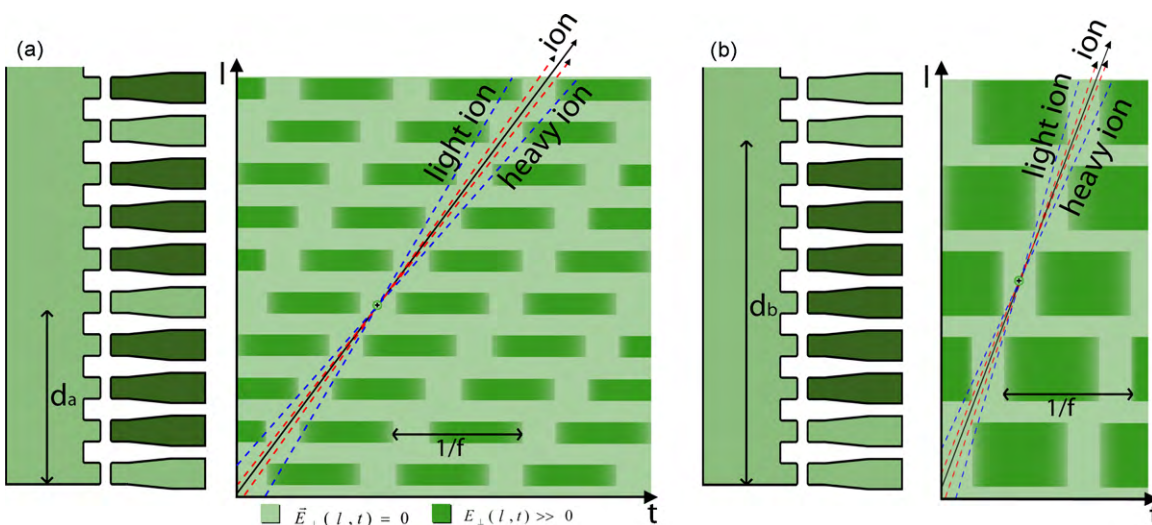


**Fig. 2.** The path-time-field diagram of the SIS mass analyzer with different electrode thicknesses. In both figures the same frequency was used. This allows different  $m/z$  to pass the SIS analyzer in both figures. (a) Finger electrodes with a distance  $d_a = 800 \mu\text{m}$  between two electrodes of the separator driven by the same signal. (b) Finger electrodes with a distance of  $d_b = 1600 \mu\text{m}$ .

The  $m/z$  ratio of ions that passes the SIS is set by varying the acceleration voltage, the signal frequency or the distance  $d$ . The increase in frequency  $f$  narrows the fields along the time axis and an increase in the width of the electrodes widens the fields along the  $d$ -axis. Both options allow for ions with higher speed to pass the separator. The slope of the ions in the diagram depends on the accelerating voltage  $U$ . For instance, ions with  $m/z$  12–1206 are measurable with an acceleration voltage of  $U = 100$  V, a distance  $d_a = 800$   $\mu\text{m}$  and a frequency range of 5–50 MHz. This is the setting hitherto used.

To detect single charged Helium ( $m/z$  4) there are three options:

- The acceleration voltage has to be reduced by at least one third. This would result in a neutralization of most of the extracted ions in the SIS mass analyzer due to thermal scattering and lead to a significant decrease in ion current. Therefore this method is not preferred.
- The frequency  $f$  has to be increased by at least factor  $\sqrt{3}$ . This is the preferred method, which is presently not possible with the current signal generator.
- The distance  $d$  has to be increased by at least factor  $\sqrt{3}$ . Fig. 3 shows a plot with the dependence of reachable  $m/z$  on  $d$ .

In this investigation, the distance  $d$  of the PIMMS was increased by factor 2 such that the detectable  $m/z$  range was shifted from the original  $m/z$  12–1206 to  $m/z$  3–301. The distance  $d$  was doubled from 800  $\mu\text{m}$  to 1600  $\mu\text{m}$ . This was done by connecting each signal of the generator to two neighbored electrodes. Fig. 2b shows how the path-time-field diagram changes using the same frequency allowing an ion with a smaller  $m/z$  to pass through the SIS.

#### 4. Results and discussion

Two different experiments were conducted using two different PIMMS chips. These chips differed from each other in their electrode width (Fig. 2). The measured spectra of both experiments

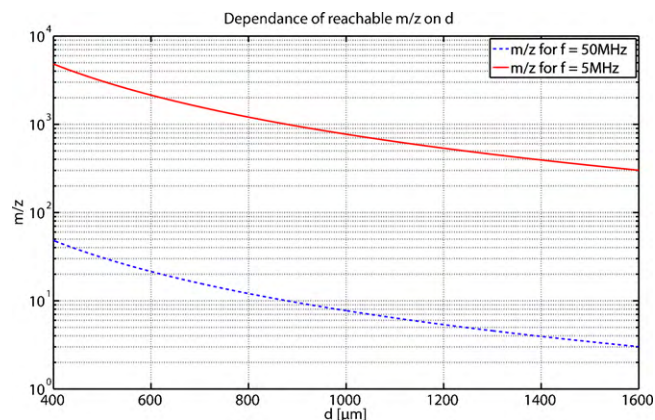


Fig. 3. Dependence of reachable  $m/z$  on the distance of the electrodes driven by the same signal of the generator.

are shown in Fig. 4. To make a statistically valid assessment of the resolution of the device, the ratio  $m/\Delta m$  (resolution) of the peaks in every spectrum was averaged and its standard deviation calculated. Spectrum 1 shows an air spectrum using  $d = 800$   $\mu\text{m}$  (O, N, H<sub>2</sub>O, N<sub>2</sub>, O<sub>2</sub>, Ar). A xenon ( $m/z$  131 and  $m/z$  65) rather than an argon plasma was used as electron source to avoid interference with the argon peak present in air. The resolution of the spectrum at FWHM is 32 with a standard deviation of 5. The scan range is trimmed down to  $m/z$  12–140 because no peaks are expected above  $m/z$  131. With  $d = 800$   $\mu\text{m}$ ,  $m/z$  12 is the lowest possible mass-to-charge ratio to be detected. Air has a concentration of 0.04% carbon dioxide ( $m/z$  44). CO<sub>2</sub> is shown in the spectrum, so the sensitivity is better than 400 ppm. The incorporated MCP allows for this high sensitivity. Spectrum 2 is measured with  $d = 1600$   $\mu\text{m}$  and an argon plasma ( $m/z$  40 and  $m/z$  20) as electron source. The sample gas is helium. Similar to Spectrum 1, the scan range is trimmed down to  $m/z$  3–70 because no peaks are expected above  $m/z$  40. The res-

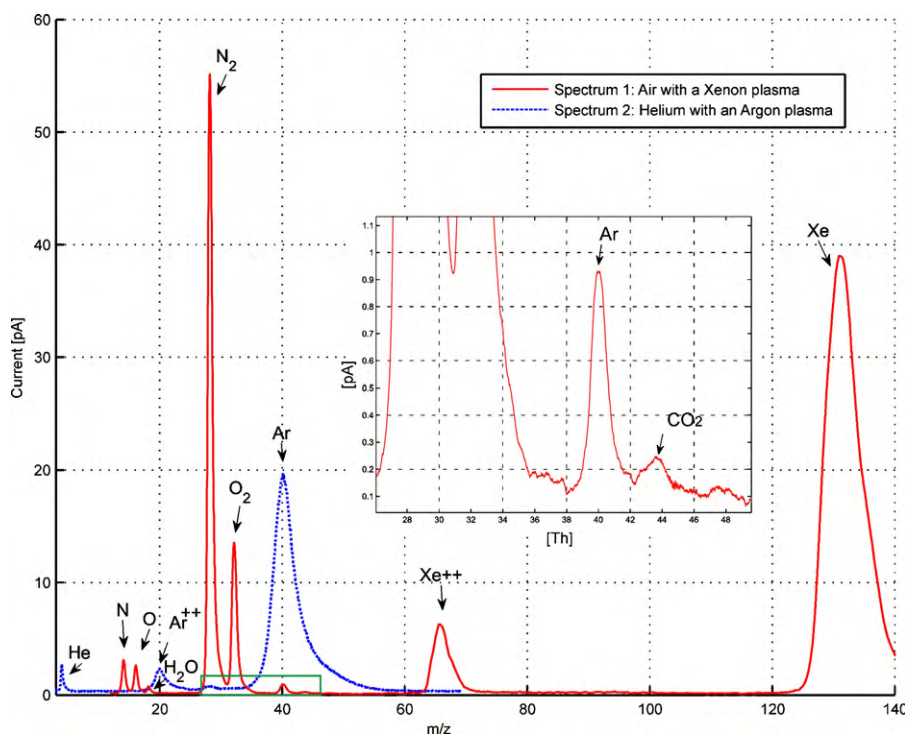


Fig. 4. Two spectra measured with two different experiments using two different PIMMS chips. Spectrum 1 shows air and xenon. Air contains N, O, H<sub>2</sub>O, N<sub>2</sub>, O<sub>2</sub>, Ar. Spectrum 2 shows He and Ar.

olution of the spectrum at FWHM reduces to 9 and its standard deviation is 1. As theoretically calculated, a distance  $d = 1600 \mu\text{m}$  enables the detection of helium ( $m/z$  4). We believe that the lower resolution of spectrum 2 is due to the wider electrodes of the SIS. As described previously, the signal generator has 4 outputs and the SIS mass analyzer is composed of 20 finger electrodes. This results in an even load of the signal generator outputs (5 electrodes per output). By coupling neighboring electrodes, the effective number of electrodes is reduced down to 10. This means 2 outputs drive 3 electrodes and 2 outputs drive 2 electrodes. The uneven load of the generator results in inhomogeneous perpendicular electric fields along the SIS. Ions which are not expected to pass the SIS at a given frequency are less deflected and yet reach the detector, directly affecting the resolution of the device.

## 5. Conclusions and outlook

The PIMMS has proven to be a versatile device. Its  $m/z$  range can be shifted according to the desired application e.g., by widening the finger electrodes of the SIS mass analyzer. This modification allowed for shifting the range of the PIMMS from  $m/z$  12–1206 to  $m/z$  3–301. A spectrum showing the presence of helium in the sample confirms the theoretical analysis. A paramount development to improve both the resolution and the  $m/z$  scan range of the PIMMS will be to increase the operating frequency of the SIS mass analyzer.

## Acknowledgements

Bayer Technology Services (BTS) and Krohne Messtechnik GmbH are acknowledged.

This research and development project is funded by the German Federal Ministry of Education and Research (BMBF) within the Framework Concept “Research for Tomorrow’s Pro-

duction” (02PC2100) and managed by the Project Management Agency Forschungszentrum Karlsruhe, Production and Manufacturing Technologies Division (PTKA-PFT).

## References

- [1] S.A. Lammert, A.A. Rockwood, M. Wang, M.L. Lee, E.D. Lee, S.E. Tolley, J.R. Oliphant, J.L. Jones, R.W. Waite, Miniature toroidal radio frequency ion trap mass analyzer, *Journal of the American Society for Mass Spectrometry* 17 (2006) 916–922.
- [2] D.E. Austin, Y. Peng, B.J. Hansen, I.W. Miller, A.L. Rockwood, A.R. Hawkins, S.E. Tolley, Novel ion traps using planar resistive electrodes: Implications for miniaturized mass analyzers, *Journal of the American Society for Mass Spectrometry* 19 (2008) 1435–1441.
- [3] L. Gao, G. Li, Z. Niea, J. Duncana, Z. Ouyangb, R.G. Cooks, Characterization of a discontinuous atmospheric pressure interface. Multiple ion introduction pulses for improved performance, *International Journal of Mass Spectrometry* 283 (2009) 30–34.
- [4] J.A. Diaz, C.F. Giese, W.R. Gentry, Sub-miniature ExB sector field mass spectrometer, *American Society for Mass Spectrometry* 12 (2001) 619–632.
- [5] S. Taylor, R.F. Tindall, R.R.A. Syms, Silicon based quadrupole mass spectrometry using micro-electromechanical systems, *Journal of Vacuum Society and Vacuum B* 19 (2) (2001) 557–562.
- [6] L.F. Velásquez-García, K. Cheung, A.I. Akinwande, An application of 3-D MEMS packaging: out-of-plane quadrupole mass filters, *Journal of Microelectromechanical Systems* 17 (6) (2008) 1430–1438.
- [7] B. Brkić, N. France, A.T. Clare, C.J. Sutcliffe, P.R. Chalker, S. Taylor, Development of quadrupole mass spectrometers using rapid prototyping technology, *Journal of the American Society of Mass Spectrometry* 20 (2009) 1359–1365.
- [8] J.-P. Hauschild, E. Wapelhorst, J. Müller, Mass spectra measured by a fully integrated MEMS mass spectrometer, *International Journal of Mass Spectrometry* 264 (2007) 53–60.
- [9] E. Wapelhorst, J.-P. Hauschild, J. Müller, Complex MEMS: a fully integrated TOF micro mass spectrometer, *Sensors and Actuators A Physical* 138 (2007) 22–27.
- [10] J.-P. Hauschild, E. Wapelhorst, J. Müller, The novel synchronous ion shield mass analyzer, *Journal of Mass Spectrometry* 44 (2009) 1330–1337.